





Article

Characterization and Productivity of Alluvial Aquifers in Sustainability Oasis Areas: A Case Study of the Tata Watershed (Southeast Morocco)

Fatima Zahra Echogdali ¹, Said Boutaleb ¹, Hasna El Ayady ¹, Mohamed Aadraoui ², Kamal Abdelrahman ³ , Amine Bendarma ⁴ , Mustapha Ikirri ¹, Tamer Abu-Alam ^{5,6,*} , Mouna Id-Belqas ¹  and Mohamed Abioui ^{1,7,*}

¹ Department of Earth Sciences, Faculty of Sciences, Ibnou Zohr University, Agadir 80000, Morocco

² Laboratory of Geo-Ressources and Environnement, Faculty of Science and Technology, Sultan Moulay Slimane University, Beni Mellal 23000, Morocco

³ Department of Geology & Geophysics, College of Science, King Saud University, Riyadh 11451, Saudi Arabia

⁴ Laboratory for Sustainable Innovation and Applied Research, Universiapolis—International University of Agadir, Agadir 80000, Morocco

⁵ The Faculty of Biosciences, Fisheries and Economics, UiT the Arctic University of Norway, 9037 Tromsø, Norway

⁶ OSEAN—Outermost Regions Sustainable Ecosystem for Entrepreneurship and Innovation, University of Madeira, Colégio dos Jesuítas, 9000-039 Funchal, Portugal

⁷ MARE-Marine and Environmental Sciences Centre—Sedimentary Geology Group, Department of Earth Sciences, Faculty of Sciences and Technology, University of Coimbra, 3030-790 Coimbra, Portugal

* Correspondence: tamer.abu-alam@uit.no (T.A.-A.); m.abioui@uiz.ac.ma (M.A.)



Citation: Echogdali, F.Z.; Boutaleb, S.; El Ayady, H.; Aadraoui, M.; Abdelrahman, K.; Bendarma, A.; Ikirri, M.; Abu-Alam, T.; Id-Belqas, M.; Abioui, M. Characterization and Productivity of Alluvial Aquifers in Sustainability Oasis Areas: A Case Study of the Tata Watershed (Southeast Morocco). *Appl. Sci.* **2023**, *13*, 5473. <https://doi.org/10.3390/app13095473>

Academic Editors: Chang-Gu Lee and José Miguel Molina Martínez

Received: 27 December 2022

Revised: 26 February 2023

Accepted: 9 March 2023

Published: 27 April 2023



Copyright: © 2023 by the authors. Licensee MDPI, Basel, Switzerland. This article is an open access article distributed under the terms and conditions of the Creative Commons Attribution (CC BY) license (<https://creativecommons.org/licenses/by/4.0/>).

Abstract: Groundwater from alluvial aquifers is a critical source of water supply for rural agriculture, particularly in semi-arid and arid regions. Effective management of these aquifers requires an understanding of the factors that influence their water resources. In this study, we present a case study of the Tata watershed in southeastern Morocco, where the economy is heavily dependent on agriculture and relies exclusively on groundwater. We demonstrate the importance of integrating geological, hydrogeological, and geophysical methods to characterize the aquifer and evaluate groundwater productivity. Analysis of 64 data wells tapping into the aquifer revealed significant disparities in flow yields, ranging from 0.05 to 15.50 L per second. The highest yields were found between depths of 12 and 43 m, which correspond to the alluvium and the altered and fractured part of its substrate. The maximum alluvial thickness of 57 m was determined using geo-electrical prospecting. A piezometric map was created to define the recharge zones, which correspond to the lateral contributions of the bordering Georgian limestones, and infiltration of both rain and surface water along the Tata wadi. Since 1987, there has been a continuous drop in groundwater level, which can be attributed to the increase in irrigated areas following financial incentives provided by the Moroccan government to the agricultural sector. A proposal has been made for the construction of a recharge dam to enable the recharge of the alluvial aquifer. This development is expected to serve a dual purpose by mitigating the deleterious impacts of flooding and facilitating the gradual water infiltration of the alluvial aquifer. This case study provides insights into the hydrodynamics of the aquifer and establishes a simplified model of its functioning. These findings have important implications for the management of alluvial aquifers in similar regions.

Keywords: hydrogeology; alluvial aquifer; productivity; geo-electrical; piezometric; recharge dam; Tata watershed; Morocco

1. Introduction

The rapid evolution of water needs for economic and social activities indicates that the kingdom of Morocco is currently in a transitional phase between a period when these resources were inexhaustible and the actual state where the current shortage continues

to worsen, especially in the southern regions of the kingdom [1]. This situation is due to the increasing demand for water, the overexploitation of resources, and the shortage of natural supply due to repeated periods of drought that characterize its arid to semi-arid climate [2]. Moreover, all scientific studies show that Mediterranean countries, including Morocco, are affected by global climate change, including rising temperatures and falling rainfall [3]. A vast and deplorable waste is noticed also. On a total of 16 billion m³/year of surface water, 9 billion m³ are lost by evaporation, flowing to the sea or by existing leaks in the distribution networks [4]. As a result, and to be able to meet the expressed needs, the country's natural water resources must be enhanced, according to a coherent overall plan, taking into account the requirements for conservation, prevention, and protection, both in quantity and quality [5]. The cohesion of any project proposed in the past shows specific weaknesses due to the involvement of various natural parameters, which are generally difficult to assess and, above all, very dependent on climatic hazards and geological conditions [5]. This fact often complicates any attempt at an effective and appropriate management approach. These weaknesses are felt mainly in the watersheds of the southern regions, characterized by a high climatic contrast compared to those in the north [6].

In these regions, which are generally densely populated and whose economy depends mainly on agricultural activities, the overexploitation of groundwater leads to a secular decline in the groundwater level [7]. In addition, the continuous need to increase crop production and the introduction of more water-intensive crops puts increased pressure on these resources, leading to their decline in quantity [8] and quality. In Morocco, water consumption from irrigation is about 90% [9]. Understanding its impact on the hydrological cycle is necessary for efficiently managing groundwater resources and promoting more sustainable agriculture [10,11]. The high demand for food has shifted the practice of irrigation from surface water to deep groundwater irrigation, leading to its rapid decline [8,12,13]. Morocco's current total renewable water resources (surface and groundwater) are estimated at 29 billion cubic meters (BCM) per year [4]. The usable component is 20 billion cubic meters, of which 16 billion cubic meters is surface water and 4 billion cubic meters is groundwater. Approximately 70% of this potential is currently exploited (i.e., 11 billion cubic meters of surface water and 2.7 billion cubic meters of groundwater) [4]. The depletion of groundwater by these agricultural activities is of increasing concern to groundwater resource managers in Morocco [1,5,14].

The Tata region, located in southeastern Morocco, is currently facing the challenge of excessive exploitation of its deepwater resources, particularly those from the alluvial aquifer, due to the region's recent agricultural expansion. Agricultural activities in this region require approximately 82 million cubic meters of water (15,000 cubic meters per hectare) [15]. The annual volume of water used is 69.3 million cubic meters [15], with 8.3 million cubic meters per year (12%) from surface water and 61 million cubic meters per year (88%) from groundwater. Water balance calculations reveal a relatively significant deficit (15%) for agricultural perimeters. Furthermore, this deficit is expected to increase as agricultural space expands and will undoubtedly hinder the economic development of the region, which has already been weakened by climate change in recent decades. This deficit will be particularly noticeable in alluvial aquifers due to their easy access and high productivity [16–19].

Hence, it is of great significance to conduct hydrogeological investigations in this region, which is considered a representative example, where severe climatic conditions and water shortage are increasingly becoming prominent. These factors, in turn, impose a certain level of stringency on the living standards of the populace residing in this area. Young et al. [20] and Shishaye et al. [21] have shown the importance of these studies in the characterization of alluvial aquifers.

This research fits this perspective to characterize and update the knowledge on the productivity of alluvial aquifers of the Tata basin and to evaluate the factors that influence it. In addition, this study proposes solutions to cope with the overexploitation of water resources of the alluvial aquifer, which is currently under strong pressure due to the

increase in irrigated areas in recent years. To achieve this, an integrated approach was used, combining geological, hydrogeological, and geophysical methods to characterize the aquifer. As part of a wider effort to manage groundwater resources, this study proposes the construction of a recharge dam to replenish the Tata alluvial aquifer. The proposed recharge dam would not only help in mitigating the effects of water scarcity but also contribute to the sustainable development of the region.

2. Study Area

The Tata watershed, with an area of 2567 km², is a well-individualized hydrographical system of the Anti-Atlas mountain chain. It is situated in the province of Tata in the southeastern part of Morocco, between Lambert coordinates X (200,000 and 280,000) and Y (290,000 and 360,000) (Figure 1).

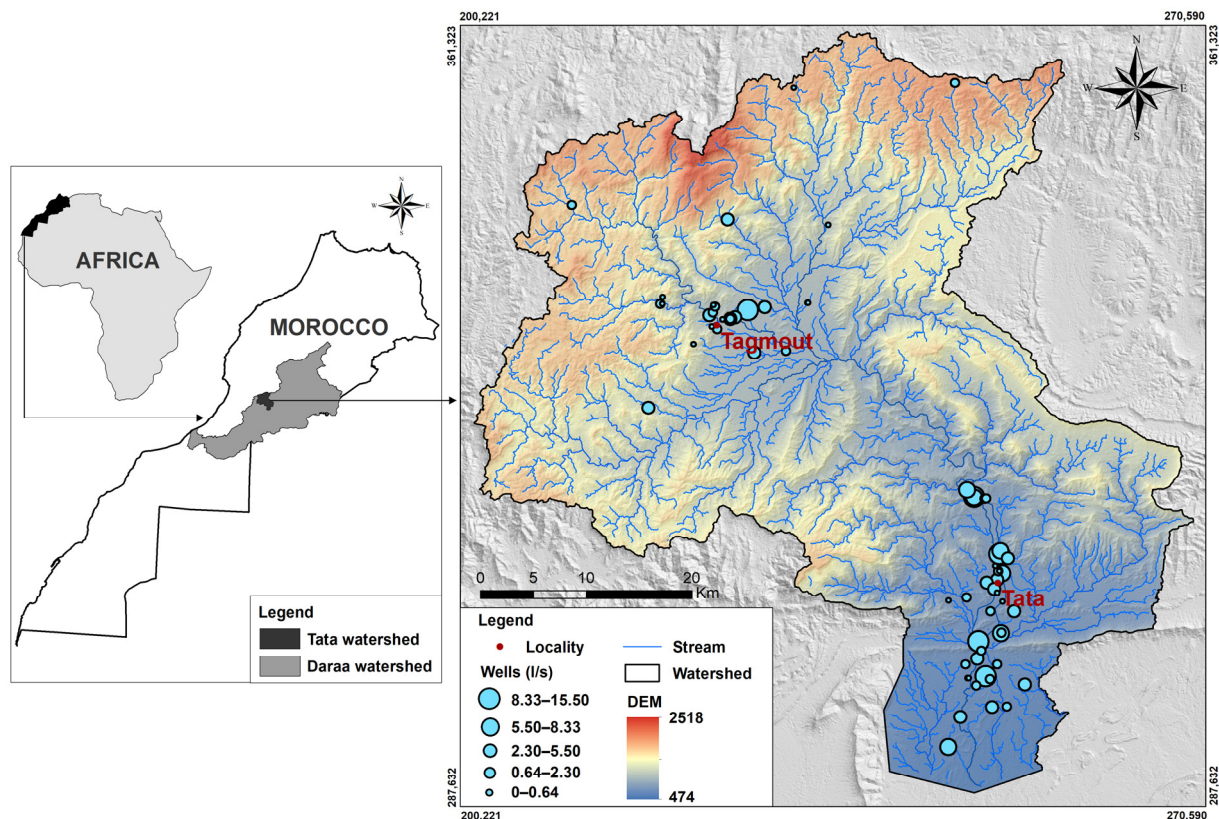


Figure 1. Location of the Tata watershed.

The climate of the basin is continental and semi-arid, with low rainfall (<150 mm/year) and high average summer temperatures (>32 °C) [22,23]. The analysis of 70-year monitoring rainfall period data shows alternate humid periods, with a duration of 8 years, followed by more extended dry periods. The range of daily and seasonal temperatures is high (19 °C in winter and 30 °C in summer). The wet period is between October and March, and the dry one can extend from April to September. The average relative moisture values show significant monthly variations, exceeding 40% in summer. They are over 40% in November, December, January, and February, when low temperatures (<16 °C) are registered.

The Tata watershed is compact, with a Gravelius Index of 1.84, and is characterized by a dense drainage network [24]. About 18 tributaries from the mountain ranges on either side of the valley contribute significantly to the flow of the Wadi Tata. The contribution from springs is very low (<1 m³/s). The monthly discharge of Wadi Tata is highly variable, because of the large variability in rainfall in the basin.

In economic terms, agriculture is the main activity in the region, with 5500 hectares of irrigated land [15]. It is developed at the oases where traditional palm groves are irrigated from alluvial aquifers by khetaras, wells, and resurgences [24,25] (Figure 2).



Figure 2. The oasis of the Tata region (photo credit: Echogdali, 2018).

Geologically, the basin is occupied by Precambrian formations composed of granite, gabbro, and schist at the Ighrem, Tagragra, and Agouliz inliers (Figure 3a). The Paleozoic cover occupies a large part of the basin, including volcano-sedimentary deposits progressing to carbonate deposits of “Lower limestones” topped with pelites of a purplish-red color “Lie-de-vin” followed by carbonate deposits of “Upper limestones” and schists–calcareous series [26–34]. Sandstones and quartzites of the Ordovician age occupy the southern part of the basin, followed by Devonian shale and limestone [35,36]. Alluvial deposits fill the valleys and form alluvial aquifers [23] (Figures 3b and 4). Structurally, three major fault directions exist in the basin: NNE–SSW, NE–SW, and E–W [27] (Figure 3a). NE–SW sills and doleritic dykes related to the opening of the Atlantic Ocean in the Triassic/Lias period traverse all these terrains [37].

From a hydrogeological perspective, the Tata watershed can be described as a series of parallel ridges intersected by two significant cluses, Tagmout in the north and Tata in the south, which are separated by plains known as Feijas. The Quaternary alluvial filling overlays the Hercynian bedrock in these Feijas (Figure 5), containing water tables that are primarily utilized for irrigating palm groves. Recharge of the alluvial aquifer occurs mainly through flooding, precipitation, and underground contributions from adjacent plain filling formations, in direct contact with the Adoudounian limestone formations. The marginal limestone formations upstream of the cluses represent ideal recharge zones for the alluvial groundwater due to their highly extensive, fractured, and fissured characteristics. These formations infiltrate precipitation to supply the underflow of the deep valleys.

Apart from the alluvial formations, the basin is dominated by discontinuous aquifers, as illustrated in Figure 3b, which possess nearly identical hydrogeological parameters. In comparison with the alluvial aquifer, the groundwater storage of these formations is insignificant. In these discontinuous aquifers, groundwater is primarily stored in fractures and crushed zones and circulates within a network of high hydraulic conductivity zones. Discharge of groundwater takes place in river valleys and depressions.

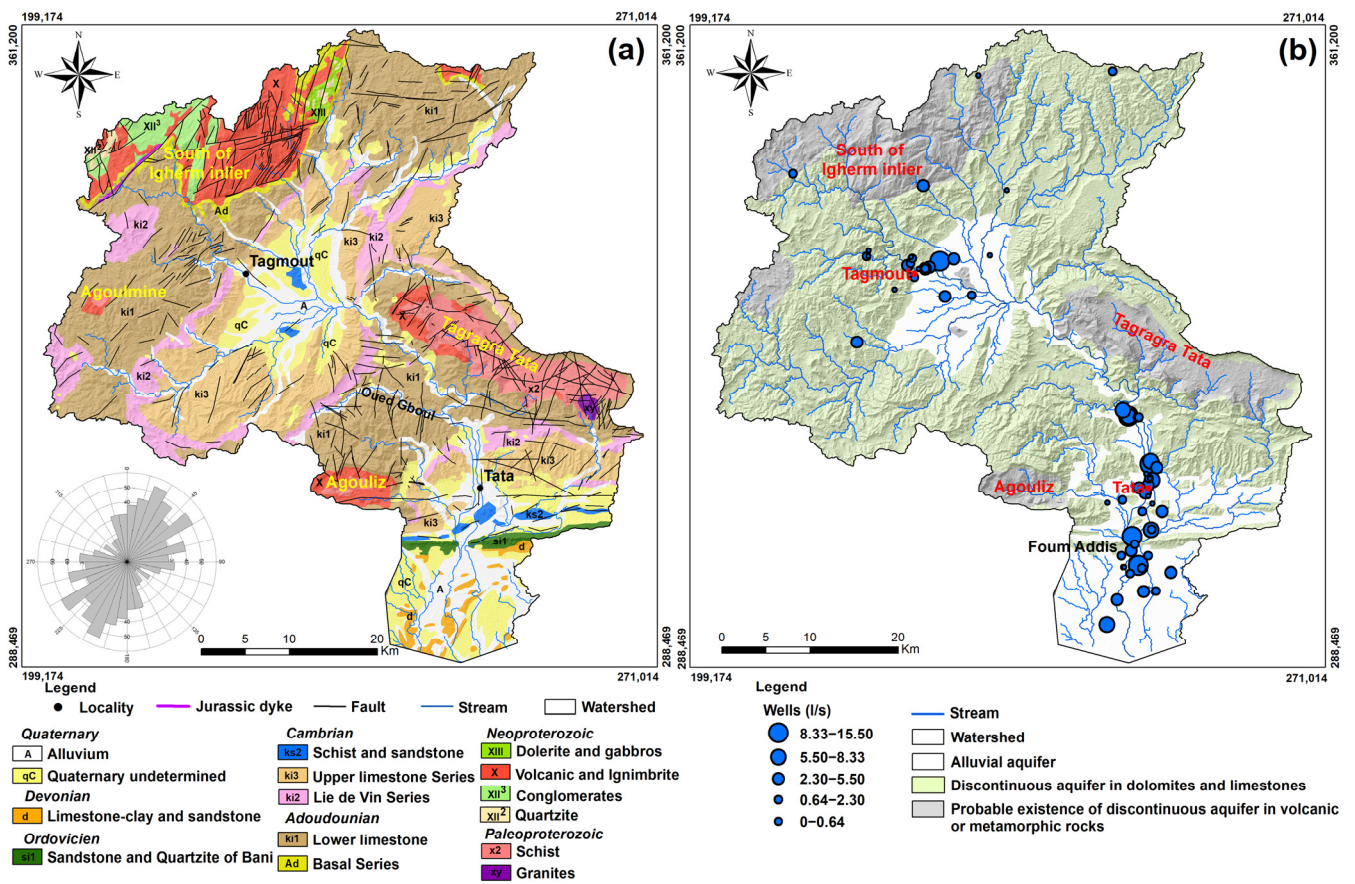


Figure 3. (a) Geological map of the Tata watershed; and (b) Map of different types of aquifer systems in the study area.

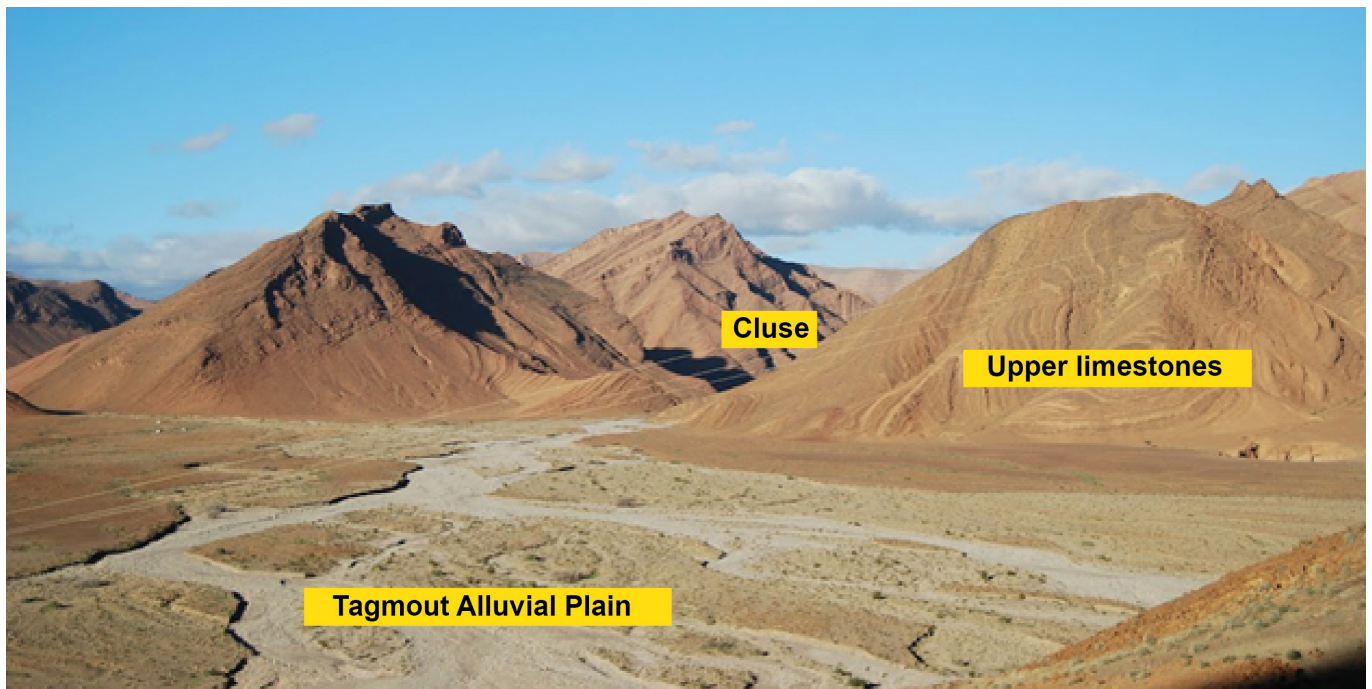


Figure 4. Some geological and geomorphological elements of the Tata watershed (photo credit: Echgdali, 2018).

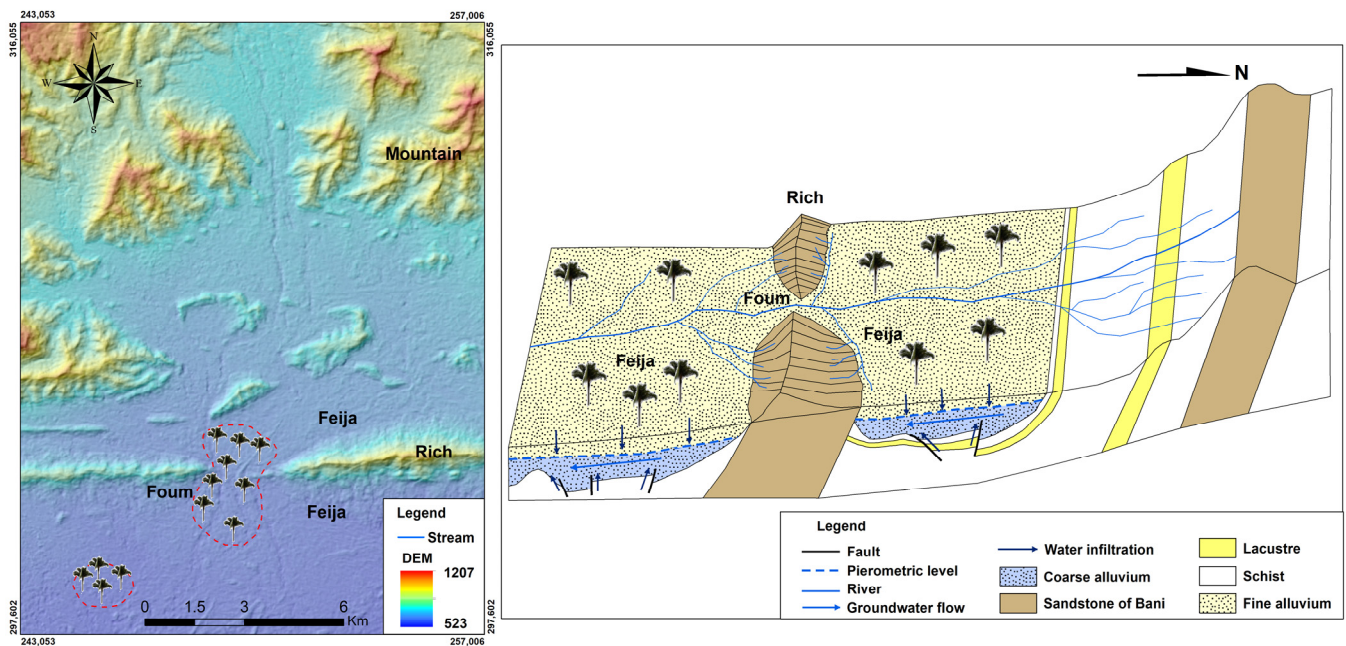


Figure 5. Hydrogeological functioning model of the groundwater alluvial in the Tata region.

3. Materials and Methods

The methodology employed in this study was based on assessing the correlation between well yield and well depth with the underlying geological formations. To achieve this, a geological map of Morocco was edited in a Geographic Information System (GIS) at a scale of 1:500,000, obtained from the Moroccan Ministry of Energy and Mines. Topographic maps were generated from a Digital Elevation Model (DEM) with a spatial resolution of 30 m, downloaded from the United States Geological Survey (USGS) website (<http://earthexplorer.usgs.gov/>, accessed on 14 December 2022). The drainage network was also derived from the DEM data (Table 1).

Table 1. Database of the Tata basin.

Category	Data Type	Resolution	Source
Topographical	Raster	30 m × 30 m	DEM (http://earthexplorer.usgs.gov/) (accessed on 14 December 2022))
Drainage network	Raster	30 m × 30 m	DEM (http://earthexplorer.usgs.gov/) (accessed on 14 December 2022))
Geological	Raster	1:500,000	Geological map of Morocco (Ministry of Energy and Mines of Morocco)
Geophysical	Raster	-	
Well	Vector	-	The Drâa-Oued Noun Hydraulic Basin Agency (Agadir, Morocco)

Hydrogeological data, including well flows, the resistivity of geological formations, and groundwater piezometric levels, were extracted from borehole logs of 64 wells, obtained from the Drâa-Oued Noun Hydraulic Basin Agency, and tracked from 1970 up to the present time. Furthermore, flood data were used to estimate extreme flows for sizing the future recharge dam to promote water infiltration in the alluvial aquifer.

In addition, a geophysical survey was conducted in the northern part of Tata city to evaluate the recharge capacity of the alluvial deposits by the recharge dam. The survey was conducted in November 2017 using the Schlumberger configuration with a maximum current electrode spacing of 250 m, which yielded the apparent electrical resistivity (ρ_a , Ω m) at different depths of the soil. Fifteen Vertical Electrical Soundings (VES) were executed and distributed across three profiles. The Schlumberger configuration was selected due to its better resolution, greater probing depth, and less time-consuming field deployment compared to other configurations [38]. The VES electrode array recorded the electrical current I applied to the outer A and B electrodes, and the potential difference ΔV was measured between the inner M and N electrodes [39–41]. The apparent resistivity ρ_a recorded by the

VES can be defined as per Flathe and Leibold [41], Telford et al. [42], and Niculescu and Andrei [43]:

$$\rho_a = K \cdot \Delta V / I \tag{1}$$

where: ρ_a = Apparent resistivity (Ohm.m); ΔV = Potential difference (mV); I = Current intensity (mA); K = Geometrical electrode factor (Equation (2)).

$$K = [2\pi / (1/AM - 1/AN - 1/BM + 1/BN)] \tag{2}$$

The quantitative interpretation of the measurements, previously plotted on a bi-logarithmic diagram, begins with smoothing the curves. Automatic processing is then utilized to perform data inversion, allowing the geophysicist to obtain the correct model through successive approximations until the identification of geological layers. The comparison of these results with well data enables a reasonable estimation of the true resistivities. It is important to note, however, that the theoretical interpretation presented in this scheme assumes that the geological formations explored are tabular, isotropic, and have sufficient resistivity contrast between them [43].

4. Results and Discussion

4.1. Well Location

Various factors have been studied to understand their impact on well productivity, including well depth, lithotypes, geological structures, topographic settings, and weathering thickness. When analyzing the flow rates of wells, it was found that they ranged from 0 to 15.50 L per second, as shown in Figure 6a. A majority of the wells (56.83%) fell in the very-low-to-low-rate category (0–3 L/s), while 18.4% were in the moderate category (3–5 L/s), 15.3% in the high category (5–10 L/s), and 9.47% in the very high category (>10 L/s). These results suggest that half of the wells had a flow rate below 3 L/s. Higher flows were observed in wells located close to perennial streams (<300 m) (Figure 3b), where the deposits were thick, permeable, and ideal for water infiltration. These geomorphological locations were suitable for shallow wells, especially for irrigation purposes, as noted in previous studies [33,34,44,45].

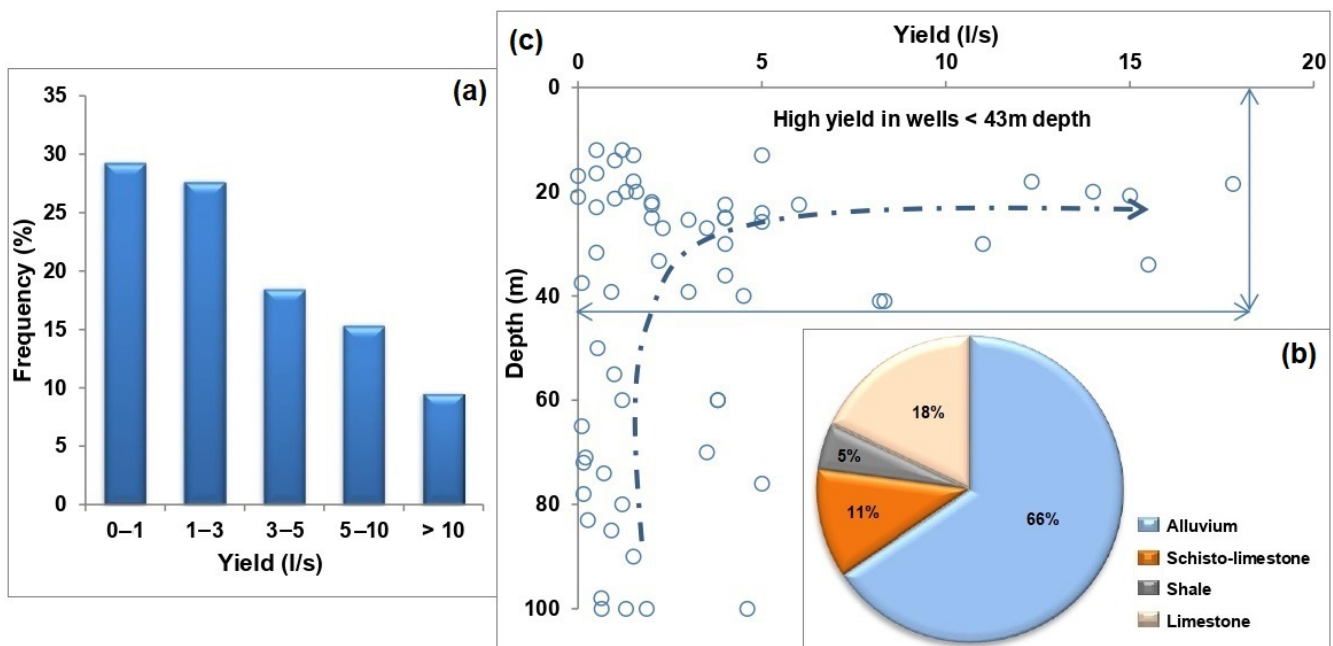


Figure 6. (a) Frequency histograms of wells yield (L/s) for the Tata watershed; (b) Percentage of wells exploiting different kinds of geological formations; and (c) Correlation between yield and depth of wells.

4.2. Factors Influencing the Productivity of Wells

4.2.1. Rock-Type Impact

To investigate the impact of rock type on well productivity, specific capacity values were categorized into two main groups: alluvial and hard rock types. Analysis of the relationship between well productivity and the geological nature of the rocks revealed that alluvium (66%) was the most productive formation, followed by limestones (17%), shales (9%), and schistose limestones (8%) (Figure 6b).

Alluvial sediments are known for their high permeability properties, as evidenced by various studies [17,44–54]. Many paleochannels have been identified as subsurface counterparts of surface rivers or creeks, and water circulation in these subsurface aquifers follow preferential flow paths within alluvial deposits [55]. These flow paths can occur in both saturated and unsaturated soils and play a critical role in groundwater flow [56,57].

On the hydrodynamic level, pumping tests conducted in the alluvial aquifer show values of transmissivity ranging from $4 \times 10^{-3} \text{ m}^2/\text{s}$ to $7 \times 10^{-4} \text{ m}^2/\text{s}$, with an average value of $3 \times 10^{-3} \text{ m}^2/\text{s}$ in the alluvial unit upstream Tagmout and $4 \times 10^{-4} \text{ m}^2/\text{s}$ in the alluvial unit of Tata.

The second most common lithotype in the area, in terms of the number of wells, is limestone, which presents itself in karst form when it contains water resources. Despite its large surface area in the Tata basin (>65%), only 18% of all boreholes in the basin exploit this type of aquifer. Studies of the Moroccan karst suggest that drought is progressively impacting water resources of this aquifer type [58–65]. This problem is particularly severe in the southern regions. Ettayfi et al. [66] investigated the origin of groundwater from the lower Cambrian carbonate aquifer of the Lakhssas Plateau in the Anti-Atlas mountains of southwestern Morocco, revealing that the limited water resources in this semi-arid zone of Morocco may be less renewable in some parts.

The third formation is schist, it contains intercalations of carbonates and quartz, as well as micaceous and clay minerals. When fractures are filled with clay or silty material, the fracture permeability is considerably reduced [67]. This may explain the low number of wells capturing this aquifer.

Statistical analysis of the parameters influencing well productivity (i.e., lithology, fracturing, and depth) has identified the optimal well depth (43 m) for good productivity. This, in addition to the influencing parameters, will depend on the renewal and recharge rate of the alluvial aquifer.

4.2.2. Wells Depth Impact

The drilled wells exhibit a total depth range of 12 to 103 m, with the highest flow rates observed at shallow depths (<43 m) and the lowest rates (<2 L/s) recorded across all depths (Figure 6c). A discernible trend in declining well productivity with increasing depth is evident. These findings regarding the influence of well depth on productivity align with previous studies conducted by Neves and Morales [68] and Douagui et al. [69], particularly for deeper wells. While they identified a decreasing tendency in well productivity with depth, the correlation coefficient between variables was relatively low. Davis and Turk [70] and Bank [71] attributed the decrease in well productivity to the closure of discontinuities by lithostatic pressure, which leads to lower fracture density and connectivity with increasing depths. This explanation aligns with our study if we focus only on wells in discontinuous aquifers such as limestones, schists, and schistose limestones.

4.2.3. Hydrodynamic Properties of Alluvial Aquifers

The piezometric map, edited from the groundwater level in 2016, displayed a substantial recharge of the aquifer in the northern section of the watershed. This happened when the Georgian limestones made direct contact with the Plio-quadernary formations of the plain. Figure 7a indicates that the flow of groundwater and surface water is, generally, the same. The hydraulic gradient differs from upstream to downstream, with the lowest values (1%) found at the plain's edge, medium values (2%) by passing the "foums" zones, and

the highest values (3 to 4%) coinciding with the plain’s central axis. The primary surface water collector, which drains the central region of the plain, significantly replenishes the groundwater in this section, explaining the high gradient values in this axis. Precipitation increases were observed in the northern part of the basin, which was characterized by high elevations. The isopiez curves indicate that the outcrops at both the eastern and western edges of the plain are orthogonal to the direction of the low recharge from these regions.

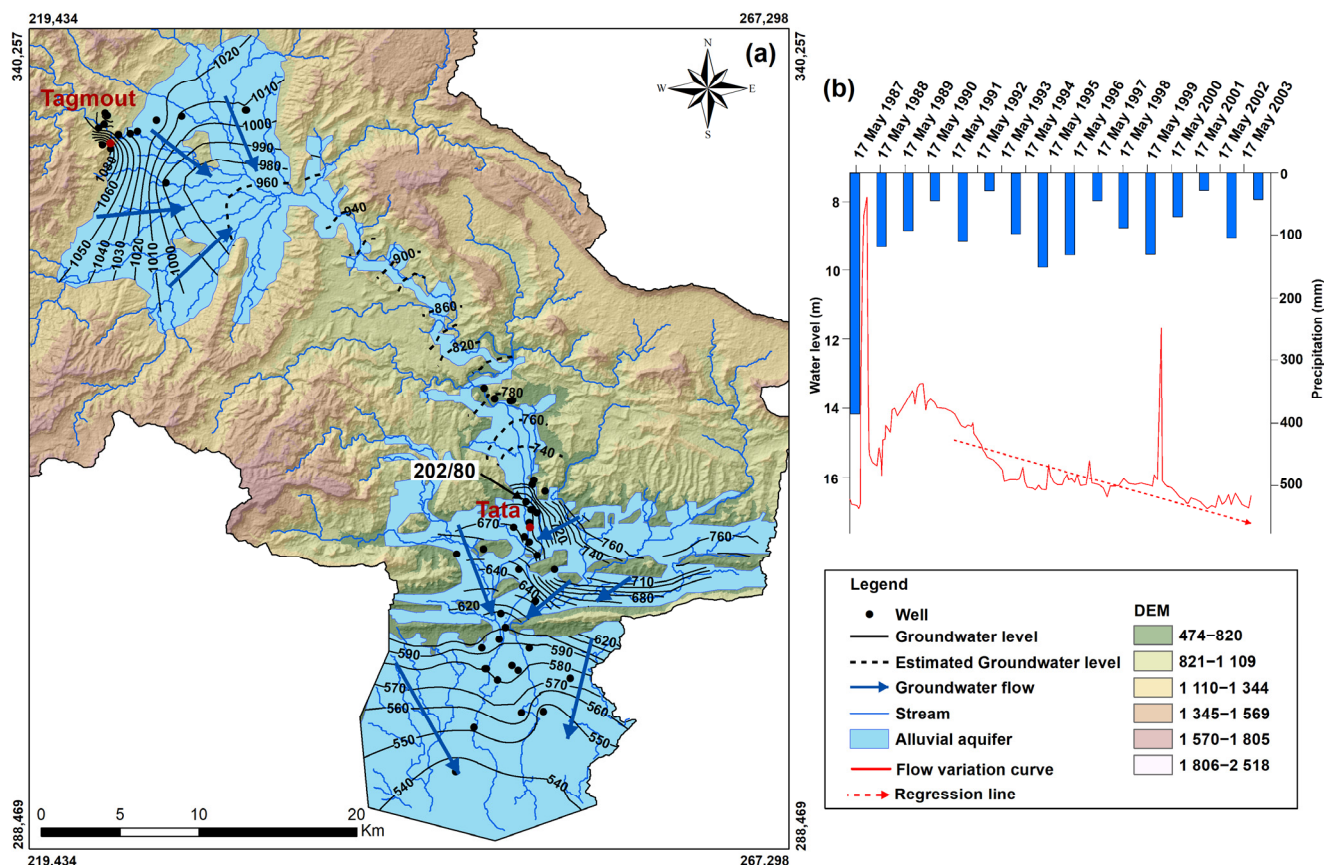


Figure 7. (a) Piezometric map of the Tata alluvial aquifer (March 2016), (b) Evolution of the water/soil level at well 202/80.

The alluvial groundwater level has declined significantly in recent years, as revealed by the monitoring of the piezometer N°202/80, which indicates a continuous drop in the water level from 1987 until 2003 (Figure 7b). A spectacular rise in groundwater level occurred during the 1999/2000 cycle following significant rainfall, but this endured only a few weeks. The level then dropped again to its initial state. The influence of gravity irrigation on the water table did not appear in this area, with high water levels in winter and spring and low water levels in summer due to drought. The decline of groundwater level can be explained by the increase in irrigated surfaces following the financial incentives of the Moroccan government to the agricultural sector within the framework of the “Green Morocco Program”, which finances the totality of the farming investments for surfaces lower than 5 ha. In addition, the significant increase in borehole authorizations in recent decades has brought overexploitation of groundwater resources. This impact has already been exemplified in several cases studied in many arid and semi-arid countries [72–77]. The overexploitation of water has resulted in an annual groundwater deficit of 8.96 L/s, as shown in the table of alluvial groundwater balances made by the Drâa-Oued Noun Hydraulic Basin Agency (2014) (Table 2).

Table 2. Alluvial groundwater balances in Tata watershed.

Groundwater Recharge (L/s)	
Infiltration of rainwater at the plain	38.5
Recharge from the edges	160
Infiltration from surface water	45.9
Reinfiltration of irrigation water taken from groundwater	22.04
Total inflow rates into the alluvial aquifer	277.44
Groundwater Discharge (L/s)	
Agricultural withdrawals and Drinking Water Supply	245.4
Water evaporation at the level of the foun	25
Downstream flow at the southern limit of the aquifer	16
Total outflow rates from the alluvial aquifer	286.4
Water balance of the alluvial aquifer	−8.96

4.3. Impact of a Proposed Recharge Dam on the Infiltration of Water on the Tata Alluvial Aquifer

4.3.1. Site Choice of the Future Recharge Dam

The mountainous basin of the Wadi Tata has been suffering from the overexploitation of its alluvial aquifer. To address this issue, we strongly advocate for the construction of a recharge dam upstream of Tata city. This dam would not only minimize the high risk of flooding but also replenish the alluvial aquifer downstream. Ten potential sites for the dam's construction were selected based on hydraulic calculations and bank topography, as illustrated in Figure 8a. The location of the dam was chosen based on the grain size analysis performed on 10 samples of alluvial deposits, where the proportion of fine particles (clays and silts) was low (<7%), which facilitates the infiltration of floodwaters into these formations. This dam is equipped with a discharge pipe of 800 mm in diameter. This allows a continuous flow rate of 4.3 m³/s to be evacuated. To estimate the alluvium's capacity to infiltrate and store water volumes, we used the geoelectric exploration method, as shown in Figure 8b.

The sizing of the forthcoming dam was conducted through the utilization of the ECRET software. By utilizing the hydraulic continuity equation, the balance of volumes at the inlet and outlet of the dam can be modeled during a specific time interval. This enables the determination of the water volume and level reached within the dam, as well as the requisite duration and corresponding volumes at the dam's valve outlet. Estimation of flooding at a 200-year return period was achieved through statistical adjustment of the maximum flows recorded at the Kasbat Zolite station.

Consequently, the maximum reservoir height of 9 m (775 m) (Figure 8d), based on the yield flood of a 200-year return period, permits storage of 1,620,000 m³, occupying an area of 812,000 m² (Figure 8a).

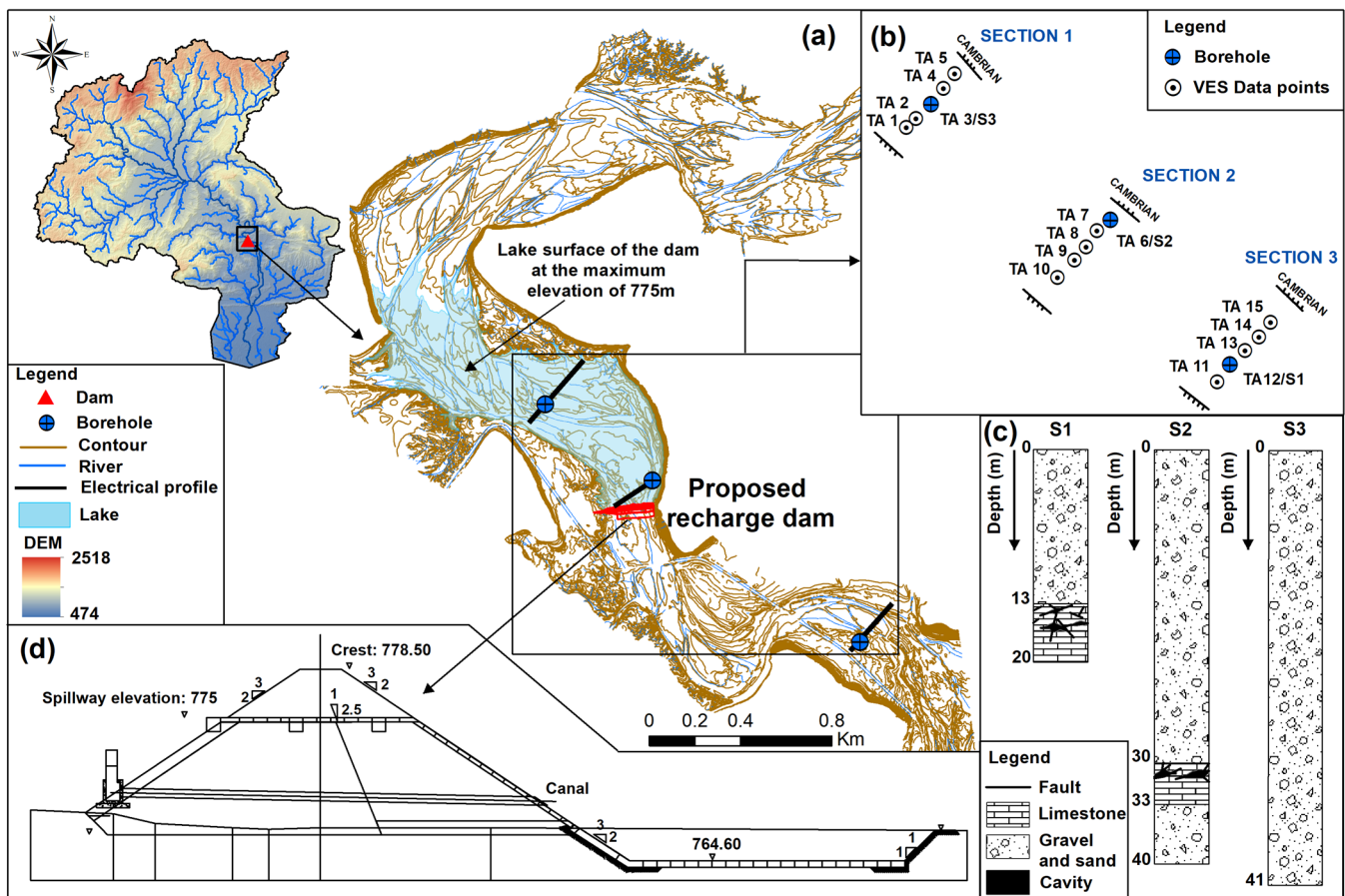


Figure 8. (a) Topographic detailed map of the geophysical prospecting profiles and location of proposed recharge dam, (b) Locations of VES stations, (c) Borehole lithology description, and (d) Architectural plan of recharge dam.

4.3.2. Geo-Electrical Methods for Estimating the Volume of Alluvial Deposits

To assess the maximum potential for the artificial recharge of alluvial deposits in the event of the construction of a future recharge dam, fifteen vertical electrical surveys (VES) were conducted in the northern region of Tata city along three parallel profiles (Figure 8b). The geological interpretation of these VESs was based on information obtained from mechanical boreholes S1, S2, and S3 (Figure 8c). All VES graphics were found to be part of the same family, as demonstrated by TA3, TA6, and TA12 (VESs) conducted in the vicinity of S3, S2, and S1 boreholes, respectively (Figure 9). Based on outcrop observations, the bedrock of the alluvial aquifer is believed to be composed of Cambrian shale and sandstone. The analysis of the TA3 VES indicates the presence of the following:

- A resistant set R_o , consisting of alternating conductive and resistant layers that represent the dry and heterogeneous alluvium (containing intercalations of clayey sands).
- A deep conductor C_p , corresponding to the saturated which corresponds to alluvium shows alternating layers of limestone.
- A resistant substratum R_s , attributed to the sandstone formations with schistous intercalations.

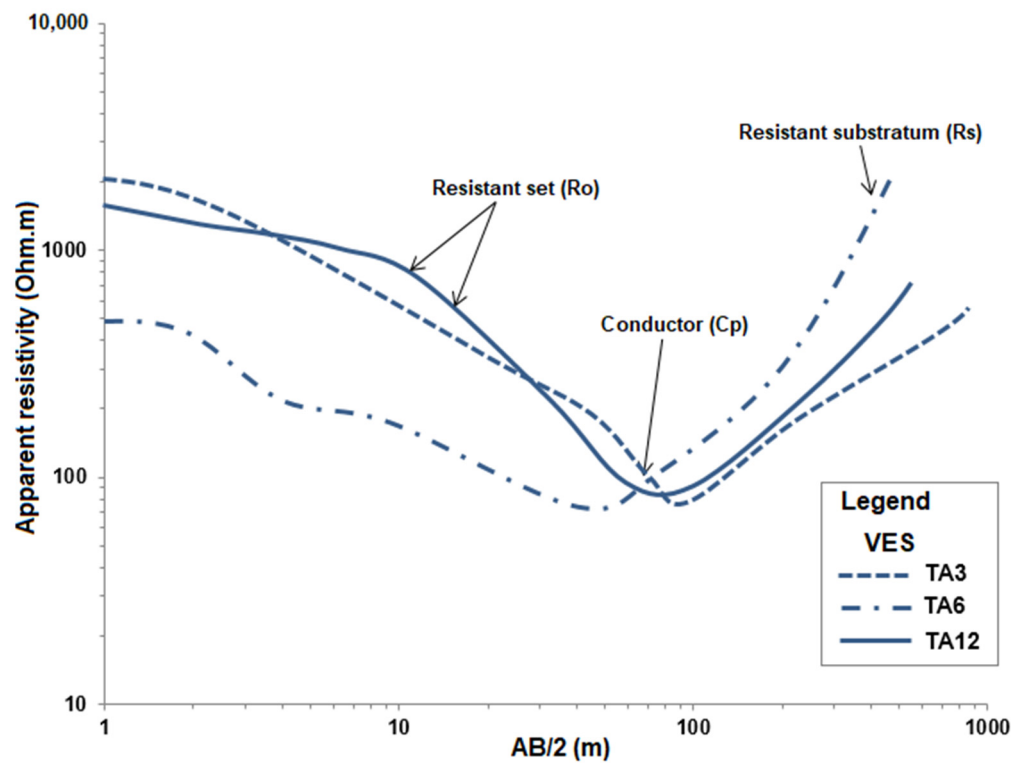


Figure 9. Electrical survey family graphics.

The results of the introduced seven-layer model in the WinSev software for all VESs are summarized in Table 3.

Table 3. Model optimization results of TA3 VES.

Layer	Layer Designation	Resistivity (Ohm.m)	Thickness (m)	Roof Depth of the Layer (m)
1		1682.75	2.08	0
2		340.55	2	−2.08
3	Ro	893.41	2	−4.08
4		172.15	4	−6.08
5		1389.47	4	−10.08
6	Cp	29.02	36	−14.08
7	Rs	1195.41	inf.	−50.08

Standard deviation= 3.166472^{-2} , Max Relative Error = 6.83%, Number of iterations = 10.

4.3.3. Geoelectrical Cross-Sections

- Section 1 shows alternating resistive and conductive layers (Figure 10). The alluvium formations above the piezometric level (PL) are resistant. Those below the PL have low resistivity whose origin can be due to the impact of water or, possibly, the existence of clayey elements in this layer. The resistant bedrock, not reached by the mechanical borehole S3, is estimated at a depth of 41, 50, and 52 m at TA5, TA3, and TA4 VESs. This geo-electrical section shows this alluvial aquifer’s significant potential (average of 50 m).
- Section 2 shows a less resistant cover above the PL than Section 1. It, possibly, corresponds to limestone and lacustrine clay. The top of this resistant layer deepens slightly from SW to NE.
- Section 3 shows a slight dip of the bedrock from SW to NE, reaching a depth of about 57 m at TA14 VES.

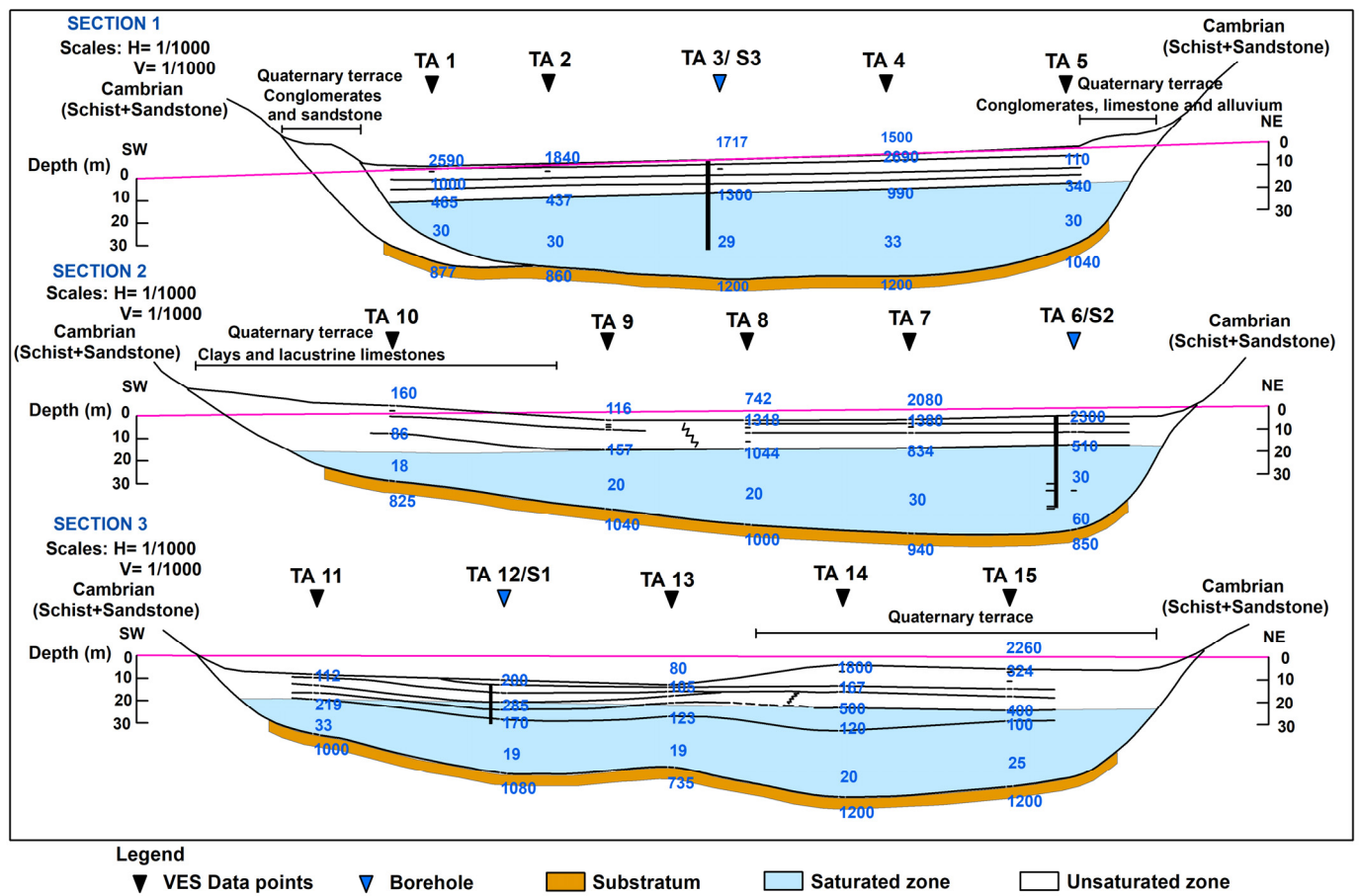


Figure 10. Geo-electrical sections deduced from the interpretation of the VES.

Table 4 summarizes the thickness of the alluvium in the upstream region of Wadi Tata.

Table 4. Thickness of the alluvium according to the vertical electrical soundings.

Section	VES	Thickness of the Alluvium (m)	Average Thickness (m)
1	TA1	41	46
	TA 2	44	
	TA 3/S3	50	
	TA 4	52	
	TA 5	42	
2	TA 6/S2	48	42
	TA 7	48	
	TA 8	44	
	TA 9	38	
	TA 10	32	
3	TA 11	26	42
	TA 12/S1	41	
	TA 13	35	
	TA 14	57	
	TA 15	50	

4.3.4. Modeling the Infiltrated Water Volumes by the Effect of the Future Recharge Dam

The alluvial formations that will be subject to artificial recharge by the dam correspond to the alluvial deposits located just upstream of the dam, more precisely the areas that will be occupied by water when it is accumulated within the dam, and those located downstream of it when the water is released through the dam’s discharge pipe.

The horizontal permeability measured in the alluvial deposits of the Wadi Tata is 10^{-3} m/s, corresponding to an infiltration rate of 1.5 m/day. Moreover, the analysis of the results obtained by the Souss Hydraulic Basin Agency on the releases from the Aoulouz dam for the recharge of the Souss river basin provides an infiltration rate of about 1 m/d. Given the similarity between the physical characteristics of the alluvial deposits of the Tata and Souss rivers and the correspondence of the calculated permeability values in both areas, the adopted infiltration rate is 1 m/day = 0.04 m/h.

To evaluate the effect of the planned dam on infiltration in the aquifer, the flood recorded at the Kasba Zolite station on 10 November 1988 was chosen. This flood is characterized by a very sharp and pointed hydrograph, which shows a rise time of 3 h with a peak flow of 277 m³/s, and the recession, which is generally slower, lasted several hours. The flood had a duration of 31 h, an average flow rate of 46.6 m³/s, and a total water volume of 5.2 million m³.

Volume of Water Infiltrated in the Absence of the Future Dam

The infiltration calculation was carried out for the section of the recharge dam, which includes the upstream basin and downstream alluvial aquifer. The section has a total length of 3575 m, with an area of 812,000 square meters, and an average width of approximately 230 m. However, during a flood, the water only uses the active beds of the river with an average width of about 50 m. The infiltration rate into the alluvium was calculated based on the water–alluvium contact surface area, which is 178,500 square meters (Table 5).

Table 5. Results of the calculation of the infiltrated water volumes in absence of a dam.

t (h)	Q (m ³ /s)	V1 (Mm ³)	V2 (Mm ³)	V3 (Mm ³)	V4 (Mm ³)	V5 (Mm ³)	V6 (Mm ³)
0	0.0	0.0000	0.0000	0.0000	0.0000	0.0000	0.0000
0.5	73.4	0.0661	0.0036	0.0036	0.0036	0.0661	0.0625
2	277.0	0.9461	0.0108	0.0108	0.0144	1.0121	0.9977
4.5	130.0	1.8315	0.0180	0.0180	0.0324	2.8436	2.8112
7	68.4	0.8928	0.0180	0.0180	0.0504	3.7364	3.6860
10.5	30.0	0.6199	0.0252	0.0252	0.0756	4.3564	4.2808
15	16.7	0.3783	0.0324	0.0324	0.1080	4.7346	4.6266
31	0.0	0.4810	0.1152	0.1152	0.2232	5.2156	4.9924

t (h) = time (hours) of the flood. Q (m³/s) = flow rate of the flood at time t (h). V1 (Mm³) = volume of water discharged in the interval (Mm³). V2 (Mm³) = volume of water that can infiltrate in the interval. V3 (Mm³) = volume of water effectively infiltrated in the interval (Mm³). V4 (Mm³) = total volume of water infiltrated at time t. V5 (Mm³) = total volume of water in the flood at time t. V6 (Mm³) = total volume of water discharged at time t.

Results of the calculation of the infiltrated water volumes in absence of a dam are summarized in the following table. Without the dam, the flood would infiltrate 0.22 million cubic meters of water into the alluvial soil (4.2% of the total flood volume).

Estimation of Water Volumes Infiltrated in the Presence of the Future Dam

After the construction of the dam, water infiltration into the alluvium can occur either upstream or downstream in the section corresponding to the alluvial water table. To calculate the volume of water infiltrated in the presence of the future dam, it is necessary to model the different flow rates corresponding to those of the spillway, culvert, and inflow at the basin level. The results of this modeling are presented in Table 6.

Table 6. Results of the calculation of the infiltrated water volumes in presence of a dam.

h (m)	t (h)	Qinf Up (m ³ /s)	Qb+d Up(m ³ /s)	Vinf.p Up (Mm ³)	Vinf.t Up (Mm ³)	Qb+d Down (m ³ /s)	V1 Down (Mm ³)	V2Down (Mm ³)	V3Down (Mm ³)	V4Down (Mm ³)
0	0	0.000	0.000	0.000	0.000	0.000	0.000	0.000	0.000	0.000
8.32	3	6.098	89.325	0.033	0.033	89.325	0.482	0.009	0.009	0.474
8.36	6	6.154	102.161	0.066	0.099	102.161	1.034	0.009	0.018	1.499
8.16	9	5.919	47.352	0.065	0.164	47.352	0.807	0.009	0.027	2.297
8.07	12	5.811	21.899	0.063	0.228	21.899	0.374	0.009	0.035	2.662
8.03	15	5.773	12.688	0.063	0.290	12.688	0.187	0.009	0.044	2.840
8.02	18	5.755	8.442	0.062	0.352	8.442	0.114	0.009	0.053	2.945
8.01	21	5.742	5.316	0.062	0.415	5.316	0.074	0.009	0.062	3.011
7.99	24	5.721	3.214	0.062	0.476	3.214	0.046	0.009	0.071	3.048
7.90	27	5.624	3.181	0.061	0.538	3.181	0.035	0.009	0.080	3.074
7.74	30	5.435	3.119	0.060	0.597	3.119	0.034	0.009	0.089	3.099
5.81	60	3.482	2.219	0.482	1.079	2.219	0.288	0.089	0.177	3.299
4.12	90	2.099	0.205	0.301	1.380	0.205	0.131	0.089	0.266	3.341
1.92	120	0.755	0.211	0.154	1.534	0.211	0.022	0.022	0.288	3.341
0.86	150	0.290	0.144	0.056	1.591	0.144	0.019	0.019	0.307	3.341
0.39	180	0.120	0.075	0.022	1.613	0.075	0.012	0.012	0.319	3.341
0.17	210	0.052	0.035	0.009	1.622	0.035	0.006	0.006	0.325	3.341
0.08	240	0.023	0.016	0.004	1.626	0.016	0.003	0.003	0.328	3.341
0.03	270	0.010	0.008	0.002	1.628	0.008	0.001	0.001	0.329	3.341
0	300	0.000	0.000	0.008	1.631	0.000	0.006	0.006	0.335	3.341

h = height of the water level in the reservoir (meters). t (h) = time from the beginning of the flood. QinfUp = infiltration flow in the upstream of the dam basin (m³/s). Qb+dUp = flow rate of the nozzle and spillway upstream of the dam basin (m³/s). Vinf.pUp = volume of water infiltrated in the interval upstream of the dam basin (Mm³). Vinf.t Up = total volume infiltrated upstream of the dam basin (Mm³). Qb+dDown (m³/s) = flow rate of the nozzle and spillway downstream of the dam. V1 Down (Mm³) = volume of water released from the dam within the interval downstream of the dam. V2Down (Mm³) = volume of water actually infiltrated within the interval downstream of the dam. V3Down (Mm³) = total volume of water infiltrated within the interval downstream of the dam. V4Down (Mm³) = total volume of water discharged downstream of the dam.

In total, 1.6 million cubic meters of water infiltrate into the recharge dam basin and 3.6 million cubic meters of water exit from the future dam. The volume of water infiltrated into the alluvium downstream of the future dam is estimated to be 0.3 million m³ (6% of the total floodwater volume), and the volume of water flowing downstream is estimated to be 3.3 million m³ (63% of the total floodwater volume).

The application of the Ecret model on this flood shows that the comparison between the volumes infiltrated in the absence and presence of the future dam indicates the benefits of this type of structure in recharging the Tata alluvial aquifer. The rate of increase in underground reserves has been multiplied by 10, as shown in Figure 11.

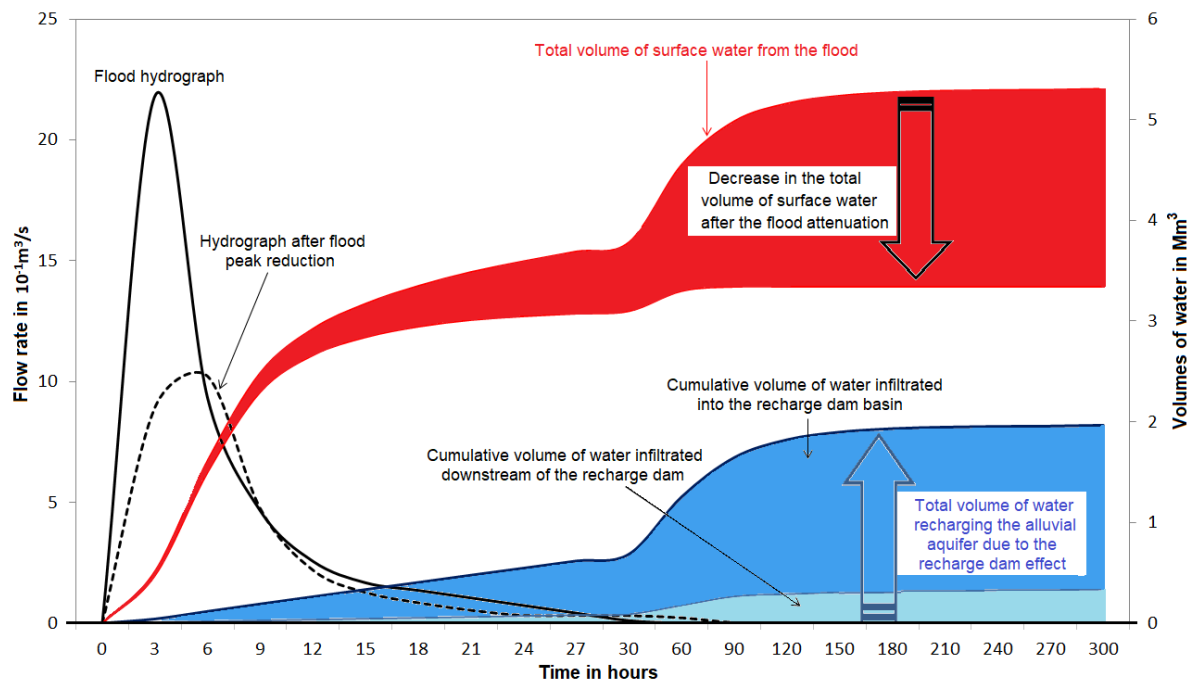


Figure 11. Comparison of water volumes in the presence and absence of the future overflow dam.

5. Conclusions

The Tata watershed is a region that contains localized alluvial groundwater in two areas, Tagmout to the north and Tata to the south. The study evaluated the factors that influence the productivity of wells by integrating geological, hydrogeological, and geophysical data in the study area.

Analysis of 64 wells showed that geological formations, such as alluvium and limestone, topography, such as being located in a valley, type of aquifer, and proximity to rivers can all affect well productivity. The most productive wells were found to be associated with shallow alluvial aquifers, with depths of less than 43 m. The study also analyzed piezometric maps to understand groundwater flows. The results indicated that the direction of groundwater flows follows that of surface water, with most of the recharge occurring during flood events. However, the study found that the groundwater level has significantly declined in recent years due to the increase in irrigated surfaces in the area. The government of Morocco has provided financial incentives to the agricultural sector, which has led to increased irrigation, resulting in the overexploitation of the alluvial groundwater.

To address the overexploitation of the alluvial groundwater, the study proposes a recharge dam north of Tata city. The results of the application of the Ecret model show the benefit of this kind of dam for the recharge of the alluvial water table of Wadi Tata. The rate of increase in underground reserves has been multiplied by 10. Additionally, a more detailed analysis of other hydrogeological units such as the basement complex, composed of Precambrian igneous and metamorphic rocks, is necessary to help locate high-yielding wells. The exploration of this type of aquifer will help alleviate the pressure on alluvial aquifers. Future studies should collect additional data and examine the relative influence of each factor on well productivity.

Overall, the study provides decision-makers with an appropriate solution to address the overexploitation of the alluvial groundwater in the Tata watershed, which includes a thorough understanding of the hydrogeological system and further exploration of groundwater using various scientific methods.

Author Contributions: Conceptualization, F.Z.E., S.B., H.E.A., M.I. and M.I.-B.; methodology, F.Z.E. and S.B.; software, F.Z.E.; validation, M.A. (Mohamed Aadraoui), K.A., A.B., T.A.-A. and M.A. (Mohamed Abioui); formal analysis, F.Z.E., S.B., H.E.A., M.I. and M.I.-B.; investigation, F.Z.E.; resources, F.Z.E. and S.B.; data curation, F.Z.E.; writing—original draft preparation, F.Z.E., S.B., H.E.A., M.I. and M.I.-B.; writing—review and editing, M.A. (Mohamed Aadraoui), K.A., A.B., T.A.-A. and M.A. (Mohamed Abioui); visualization, F.Z.E.; supervision, S.B.; project administration, M.A. (Mohamed Abioui); funding acquisition, K.A. All authors have read and agreed to the published version of the manuscript.

Funding: This research was funded by Researchers Supporting Project number (RSP2023R351), King Saud University, Riyadh, Saudi Arabia.

Institutional Review Board Statement: Not applicable.

Informed Consent Statement: Not applicable.

Data Availability Statement: Not applicable.

Conflicts of Interest: The authors declare no conflict of interest.

References

1. Sarti, O.; Otal, E.; Morillo, J.; Ouassini, A. Integrated assessment of groundwater quality beneath the rural area of R'mel, Northwest of Morocco. *Groundw. Sustain. Dev.* **2021**, *14*, 100620. [[CrossRef](#)]
2. Moksitt, A. *La sécheresse au Maroc*; Direction de Météorologie Marocaine: Casablanca, Morocco, 2000; 126p.
3. Pouffary, S.; De Laboulaye, G.; Antonini, A.; Quefelec, S.; Dittrick, L. Les Défis du Changement Climatique en Méditerranée: Transformer les Contraintes en Opportunités d'Agir, ENERGIES 2050, Report. 2016. 143p. Available online: <https://www.climate-chance.org/bibliotheque/les-defis-du-changement-climatique-en-mediterranee/> (accessed on 26 December 2022).
4. Direction de la Recherche et de la Planification de l'Eau (DRPE). *Eaux Souterraines au Maroc: Comment Concilier Satisfaction des Besoins et Développement Durable des Ressources en Eau Souterraines*; Unpublished Report; Ministère Délégué Auprès du Ministre de l'Energie, des Mines, de l'Eau et de l'Environnement Chargé de l'Eau: Rabat, Morocco, 2014; 53p.
5. Ait Kadi, M.; Ziyad, A. Integrated Water Resources Management in Morocco. In *Global Water Security: Water Resources Development and Management*; Springer: Singapore, 2018; pp. 143–163. [[CrossRef](#)]
6. Knippertz, P.; Christoph, M.; Speth, P. Long-term precipitation variability in Morocco and the link to the large-scale circulation in recent and future climates. *Meteorol. Atmos. Phys.* **2003**, *83*, 67–88. [[CrossRef](#)]
7. Shah, T.; Molden, D.; Sakthivadivel, R.; Seckler, D. The global groundwater situation: An overview of opportunities and challenges. *Econ. Political Wkly.* **2000**, *36*, 4142–4150.
8. Gautam, A.; Rai, S.C.; Rai, S.P. Impact of anthropogenic activities on the alluvial aquifers of north-east Punjab, India. *Environ. Monit. Assess.* **2020**, *192*, 527. [[CrossRef](#)]
9. Fekkoul, A.; Zarhloule, Y.; Boughriba, M.; Barkaoui, A.E.; Jilali, A.; Bouri, S. Impact of anthropogenic activities on the groundwater resources of the unconfined aquifer of Triffa plain (Eastern Morocco). *Arab. J. Geosci.* **2013**, *6*, 4917–4924. [[CrossRef](#)]
10. Siebert, S.; Burke, J.; Faures, J.M.; Frenken, K.; Hoogeveen, J.; Döll, P.; Portmann, F.T. Groundwater use for irrigation—A global inventory. *Hydrol. Earth Syst. Sci.* **2010**, *14*, 1863–1880. [[CrossRef](#)]
11. Foster, S.; Shah, T. *Groundwater Resources and Irrigated Agriculture: Making a Beneficial Relation More Sustainable*; GWP Perspectives Paper, Global Water Partnership: Stockholm, Sweden, 2012.
12. Rao, T.G.; Rao, S.Y.; Mahesh, J.; Surinaidu, L.; Dhatake, R.; Rao, G.V.; Prasad, D.M. Hydrological assessment of groundwater in alluvial aquifer region, Jalandhar district, Punjab, India. *Environ. Earth Sci.* **2015**, *73*, 8145–8153. [[CrossRef](#)]
13. Zghibi, A.; Mirchi, A.; Zouhri, L.; Taupin, I.D.; Chekirbane, A.; Tarhouni, J. The implication of groundwater development and seawater intrusion for the sustainability of a Mediterranean coastal aquifer in Tunisia. *Environ. Monit. Assess.* **2019**, *191*, 696. [[CrossRef](#)]
14. Bouchaou, L.; Tagma, T.; Boutaleb, S.; Hssaisoune, M.; El Morjani, Z.E.A. Climate Change and Its Impacts on Groundwater Resources in Morocco: The Case of the Souss- Massa Basin. In *Climate Change Effects on Groundwater Resources. A Global Synthesis of Findings and Recommendations*; Treidel, H., Martin-Bordes, J.L., Gurdak, J.J., Eds.; UNESCO, International Hydrological Programme: Paris, France, 2011; pp. 129–143. [[CrossRef](#)]
15. Direction de la Recherche et de la Planification de l'Eau (DRPE). *Etude D'actualisation du Plan Directeur D'aménagement Intégré des Ressources en Eau (PDAIRE) du Bassin Hydraulique du Draa*; Secrétariat d'Etat auprès du Ministère de l'Energie, des Mines, de l'Eau et de l'Environnement, chargé de l'Eau et de l'Environnement: Rabat, Morocco, 2008.
16. Bourg, A.C.; Bertin, C. Biogeochemical processes during the infiltration of river water into an alluvial aquifer. *Environ. Sci. Technol.* **1993**, *27*, 661–666. [[CrossRef](#)]
17. Mabee, S.B. Factors influencing well productivities in glaciated metamorphic rocks. *Groundwater* **1999**, *37*, 88–97. [[CrossRef](#)]

18. McFarlane, M.J.; Chilton, P.J.; Lewis, M.A. Geomorphological controls on borehole yields: A statistical study in an area of crystalline rocks in central Malawi. The hydrogeology of crystalline basement Aquifers in Africa. *Geol. Soc. Lond. Spec. Publ.* **1992**, *66*, 131–155. [[CrossRef](#)]
19. Henriksen, H. Relation between topography and well yield in boreholes in crystalline rocks, Sognog Fjordane, Norway. *Groundwater* **1995**, *33*, 635–643. [[CrossRef](#)]
20. Young, M.E.; De Bruijn, R.G.M.; Al-Ismaïly, A.S. Exploration of an alluvial aquifer in Oman by time-domain electromagnetic sounding. *Hydrogeol. J.* **1998**, *6*, 383–393. [[CrossRef](#)]
21. Shishaye, H.A.; Tait, D.R.; Befus, K.M.; Maher, D.T. An integrated approach for aquifer characterization and groundwater productivity evaluation in the Lake Haramaya watershed, Ethiopia. *Hydrogeol. J.* **2019**, *27*, 2121–2136. [[CrossRef](#)]
22. Echogdali, F.Z.; Boutaleb, S.; Taia, S.; Ouchchen, M.; Id-Belqas, M.; Kpan, R.B.; Abioui, M.; Aswathi, J.; Sajinkumar, K.S. Assessment of soil erosion risk in a semi-arid climate watershed using SWAT model: Case of Tata basin, South-East of Morocco. *Appl. Water Sci.* **2022**, *12*, 137. [[CrossRef](#)]
23. Echogdali, F.Z.; Boutaleb, S.; Bendarma, A.; Saidi, M.E.; Aadraoui, M.; Abioui, M.; Ouchchen, M.; Abdelrahman, K.; Fnais, M.S.; Sajinkumar, K.S. Application of Analytical Hierarchy Process and Geophysical Method for Groundwater Potential Mapping in the Tata Basin, Morocco. *Water* **2022**, *14*, 2393. [[CrossRef](#)]
24. Echogdali, F.Z.; Boutaleb, S.; Jauregui, J.; Elmouden, A. Cartography of Flooding Hazard in Semi-Arid Climate: The Case of Tata Valley (South-East of Morocco). *J. Geogr. Nat. Disast.* **2018**, *8*, 214. [[CrossRef](#)]
25. Echogdali, F.Z.; Boutaleb, S.; Elmouden, A.; Ouchchen, M. Assessing flood hazard at river basin scale: Comparison between HECRAS-WMS and food hazard index (FHI) methods applied to El Maleh basin. Morocco. *J. Water Resour. Prot.* **2018**, *10*, 957–977. [[CrossRef](#)]
26. Choubert, G. *Histoire Géologique du Précambrien de l'Anti-Atlas*; Verlag Nicht Ermitteltbar: Zürich, Switzerland, 1963; 352p.
27. Faik, F.; Belfoul, M.A.; Bouabdelli, M.; Hassenforder, B. Les structures de la couverture Néoprotérozoïque terminal et Paléozoïque de la région de Tata, Anti-Atlas centre-occidentale, Maroc: Déformation polyphasée, ou interactions socle/couverture pendant l'orogénèse hercynienne? *J. Afr. Earth Sci.* **2001**, *32*, 765–776. [[CrossRef](#)]
28. Benssaou, M.; Hamoumi, N. The western Anti-Atlas of Morocco: Sedimentological and palaeogeographical formation studies in the Early Cambrian. *J. Afr. Earth Sci.* **2001**, *32*, 351–372. [[CrossRef](#)]
29. Benssaou, M.; Hamoumi, N. Le graben de l'Anti-Atlas occidentale (Maroc): Contrôle tectonique de la paléogéographie et des séquences au Cambrien inférieur. *C. R. Geosci.* **2003**, *335*, 297–305. [[CrossRef](#)]
30. Ouchchen, M.; Boutaleb, S.; El Azzab, D.; Abioui, M.; Mickus, K.L.; Miftah, A.; Echogdali, F.Z.; Dadi, B. Structural interpretation of the Igherm region (Western Anti Atlas, Morocco) from an aeromagnetic analysis: Implications for copper exploration. *J. Afr. Earth Sci.* **2021**, *176*, 104140. [[CrossRef](#)]
31. Echogdali, F.Z.; Boutaleb, S.; Abia, E.H.; Ouchchen, M.; Dadi, B.; Id-Belqas, M.; Abioui, M.; Pham, L.T.; Abu-Alam, T.; Mickus, K.L. Mineral prospectivity mapping: A potential technique for sustainable mineral exploration and mining activities—A case study using the copper deposits of the Tagmout basin, Morocco. *Geocarto Int.* **2022**, *37*, 9110–9131. [[CrossRef](#)]
32. Ouchchen, M.; Boutaleb, S.; Abia, E.H.; El Azzab, D.; Miftah, A.; Dadi, B.; Echogdali, F.Z.; Mamouch, Y.; Pradhan, B.; Santosh, M.; et al. Exploration targeting of copper deposits using staged factor analysis, geochemical mineralization prospectivity index, and fractal model (Western Anti-Atlas, Morocco). *Ore Geol. Rev.* **2022**, *143*, 104762. [[CrossRef](#)]
33. Echogdali, F.Z.; Boutaleb, S.; Abioui, M.; Aadraoui, M.; Bendarma, A.; Kpan, R.B.; Ikerri, M.; El Mekkaoui, M.; Essoussi, S.; El Ayady, H.; et al. Spatial Mapping of Groundwater Potentiality Applying Geometric Average and Fractal Models: A Sustainable Approach. *Water* **2023**, *15*, 336. [[CrossRef](#)]
34. Echogdali, F.Z.; Boutaleb, S.; Kpan, R.B.; Ouchchen, M.; Bendarma, A.; El Ayady, H.; Abdelrahman, K.; Fnais, M.S.; Sajinkumar, K.S.; Abioui, M. Application of Fuzzy Logic and Fractal Modeling Approach for Groundwater Potential Mapping in Semi-Arid Akka Basin, Southeast Morocco. *Sustainability* **2022**, *14*, 10205. [[CrossRef](#)]
35. Abia, E.H.; Benssaou, M.; Abioui, M.; Ettayfi, N.; Lhamyani, B.; Boutaleb, S.; Maynard, J.B. The Ordovician iron ore of the Anti-Atlas, Morocco: Environment and dynamics of depositional process. *Ore Geol. Rev.* **2020**, *120*, 103447. [[CrossRef](#)]
36. Wendt, J. Disintegration of the continental margin of northwestern Gondwana: Late Devonian of the eastern Anti-Atlas (Morocco). *Geology* **1985**, *13*, 815–818. [[CrossRef](#)]
37. Sahabi, M.; Aslanian, D.; Olivet, J.L. Un nouveau point de départ pour l'histoire de l'Atlantique central. *C. R. Geosci.* **2004**, *336*, 1041–1052. [[CrossRef](#)]
38. Hassan, E.; Rai, J.K.; Anekwe, U.O. Geoelectrical Survey of Ground Water in Some Parts of Kebbi State Nigeria, a Case Study of Federal Polytechnic Bye-Pass Birnin Kebbi and Magoro Primary Health Center Fakai Local Government. *Geosciences* **2017**, *7*, 141–149. [[CrossRef](#)]
39. Soomro, A.; Qureshi, A.L.; Jamali, M.A.; Ashraf, A. Groundwater investigation through vertical electrical sounding at hilly area from Nooriabad toward Karachi. *Acta Geophys.* **2019**, *67*, 247–261. [[CrossRef](#)]
40. Mlangi, T.M.; Mulibo, G.D. Delineation of shallow stratigraphy and aquifer formation at Kahe Basin, Tanzania: Implication for potential aquiferous formation. *J. Geosci. Environ. Prot.* **2018**, *6*, 78. [[CrossRef](#)]
41. Flathe, H.; Leibold, W. *The Sounding Graph: A Manual for Fieldwork in Direct Current Resistivity Sounding*; Federal Institute for Geosciences and Natural Resources: Hannover, Germany, 1976.

42. Telford, W.M.; Geldart, L.P.; Sheriff, R.E. *Applied Geophysics*, 2nd ed.; Cambridge University Press: Cambridge, UK, 1990. [[CrossRef](#)]
43. Niculescu, B.M.; Andrei, G. Using Vertical Electrical Soundings to characterize seawater intrusions in the southern area of Romanian Black Sea coastline. *Acta Geophys.* **2019**, *67*, 1845–1863. [[CrossRef](#)]
44. Holland, M. Evaluation of factors influencing transmissivity in fractured hard-rock aquifers of the Limpopo Province. *Water SA* **2012**, *38*, 379–390. [[CrossRef](#)]
45. Dapaah-Siakwan, S.; Gyau-Boakye, P. Hydrogeologic framework and borehole yields in Ghana. *Hydrogeol. J.* **2000**, *8*, 405–416. [[CrossRef](#)]
46. Schiavo, M. Probabilistic delineation of subsurface connected pathways in alluvial aquifers under geological uncertainty. *J. Hydrol.* **2022**, *615*, 128674. [[CrossRef](#)]
47. Holland, M.; Witthüser, K.T. Evaluation of geologic and geomorphologic influences on borehole productivity in crystalline bedrock aquifers of Limpopo Province, South Africa. *Hydrogeol. J.* **2011**, *19*, 1065–1083. [[CrossRef](#)]
48. Yin, Z.Y.; Brook, G.A. The Topographic Approach to Locating High-Yield Wells in Crystalline Rocks: Does It Work? *Groundwater* **1992**, *30*, 96–102. [[CrossRef](#)]
49. Rugh, D.F.; Burbey, T.J. Using saline tracers to evaluate preferential recharge in fractured rocks, Floyd County, Virginia, USA. *Hydrogeol. J.* **2008**, *16*, 251–262. [[CrossRef](#)]
50. Barker, R.D.; White, C.; Houston, J.F.T. Borehole siting in an African Accelerated Drought Relief Project. Hydrogeology of crystalline basement aquifers in Africa. *Geol. Soc. Lond.* **1992**, *66*, 183–201. [[CrossRef](#)]
51. Dewandel, B.; Maréchal, J.C.; Bour, O.; Ladouche, B.; Ahmed, S.; Chandra, S.; Pauwels, H. Upscaling and regionalizing hydraulic conductivity and effective porosity at watershed scale in deeply weathered crystalline aquifers. *J. Hydrol.* **2012**, *416*, 83–97. [[CrossRef](#)]
52. Anaba Onana, A.B.; Ngoupayou, J.N.; Ondo, J.M. Analysis of crystalline bedrock aquifer productivity: Case of central region in Cameroon. *Groundw. Sustain. Dev.* **2017**, *5*, 66–74. [[CrossRef](#)]
53. Siddiqui, S.H.; Parizek, R.R. Hydrogeologic factors influencing well yields in folded and faulted carbonate rocks in Central Pennsylvania. *Water Resour. Res.* **1971**, *7*, 1295–1312. [[CrossRef](#)]
54. Cline, G.C. Geological Factors Influencing Well-Yields in a Folded Sandstone siltstone-Shale Terrane within the East Manhantango Creek Watershed, Pennsylvania. Master's Thesis, Pennsylvania State University, State College, PA, USA, 1968.
55. Thayer, J.B.; Ashmore, P. Floodplain morphology, sedimentology, and development processes of a partially alluvial channel. *Geomorphology* **2016**, *269*, 160–174. [[CrossRef](#)]
56. Mulligan, A.E.; Evans, R.L.; Lizarralde, D. The role of paleochannels in groundwater/seawater exchange. *J. Hydrol.* **2007**, *335*, 313–329. [[CrossRef](#)]
57. Samadder, R.K.; Kumar, S.; Gupta, R.P. Paleochannels and their potential for artificial groundwater recharge in the western Ganga plains. *J. Hydrol.* **2011**, *400*, 154–164. [[CrossRef](#)]
58. Benkaddour, A. Changements Hydrologiques et Climatiques dans le Moyen Atlas Marocain: Chronologie, Minéralogie, Géochimie Isotopique et Élémentaire des Sédiments Lacustres de Tigalmamine. Ph.D. Thesis, Université Paris-Sud, Paris, France, 1993.
59. El Khalki, Y. Les Systèmes Hydro-Karstiques du Moyen Atlas du SO: Étude Hydrologique et Hydrochimique. Ph.D. Thesis, Université de Moulay Ismail, Béni Mellal, Morocco, 2002.
60. Bakalowicz, M. Contribution de la Géochimie des Eaux à la Connaissance de L'aquifère Karstique et de la Karstification. Ph.D. Thesis, Université Paris VI, Paris, France, 1979.
61. Bakalowicz, M. Karst et ressources en eau souterraine: Un atout pour le développement des pays méditerranéens. *Sécheresse* **2010**, *21*, 319–322. [[CrossRef](#)]
62. El Baghdadi, M.; Zantar, I.; Jouider, A.; Nadem, S.; Medah, R. Evaluation of hydrogeochemical quality parameters of groundwater under urban activities—Case of Beni Mellal city (Morocco). *Euro-Mediterr. J. Environ. Integr.* **2019**, *4*, 6. [[CrossRef](#)]
63. Jong, C.; Cappy, S.; Finckh, M.; Funk, D.A. Transdisciplinary analysis of water problems in the mountainous karst areas of Morocco. *Eng. Geol.* **2008**, *99*, 228–238. [[CrossRef](#)]
64. Driouech, F. Distribution des Précipitations Hivernales sur le Maroc dans le Cadre d'un Changement Climatique: Descente d'Échelle et Incertitudes. Ph.D. Thesis, Université de Toulouse, Toulouse, France, 2010.
65. Akdim, B. Karst landscape and hydrology in Morocco: Research trends and perspectives. *Environ. Earth Sci.* **2015**, *74*, 251–265. [[CrossRef](#)]
66. Ettayfi, N.; Bouchaou, L.; Michelot, J.L.; Tagma, T.; Warner, N.; Boutaleb, S.; Massault, M.; Lgourna, Z.; Vengosh, A. Geochemical and isotopic (oxygen, hydrogen, carbon, strontium) constraints for the origin, salinity, and residence time of groundwater from a carbonate aquifer in the Western Anti-Atlas mountains, Morocco. *J. Hydrol.* **2012**, *438*, 97–111. [[CrossRef](#)]
67. Benjmel, K.; Amraoui, F.; Aydda, A.; Tahiri, A.; Yousif, M.; Pradhan, B.; Abdelrahman, K.; Fnais, M.S.; Abioui, M. A multidisciplinary approach for groundwater potential mapping in a fractured semi-arid terrain (Kerdous Inlier, Western Anti-Atlas, Morocco). *Water* **2022**, *14*, 1553. [[CrossRef](#)]
68. Neves, M.A.; Morales, N. Well productivity controlling factors in crystalline terrains of southeastern Brazil. *Hydrogeol. J.* **2007**, *15*, 471–482. [[CrossRef](#)]

69. Douagui, A.G.; Kouadio, S.K.A.; Mangoua, J.O.M.; Kouassi, A.K.; Kouam, B.K.; Savané, I. Using specific capacity for assessing of the factors controlling borehole productivity in crystalline bedrock aquifers of N’Zi, Iffou and Moronou regions in the eastern area of côte d’Ivoire. *Groundw. Sustain. Dev.* **2019**, *9*, 100235. [[CrossRef](#)]
70. Davis, S.N.; Turk, L.J. Optimum depth of wells in crystalline rocks. *Groundwater* **1964**, *22*, 6–11. [[CrossRef](#)]
71. Banks, D. Optimal orientation of water-supply boreholes in fractured aquifers. *Groundwater* **1992**, *30*, 895–900. [[CrossRef](#)]
72. Böhlke, J.K. Groundwater recharge and agricultural contamination. *Hydrogeol. J.* **2002**, *10*, 153–179. [[CrossRef](#)]
73. Flury, M. Experimental evidence of transport of pesticides through field soils—A review. *J. Environ. Qual.* **1996**, *25*, 25–45. [[CrossRef](#)]
74. Zaporozec, A.; Conrad, J.E.; Hirata, R.; Johansson, P.O.; Nonner, J.C.; Romijn, E.; Weaver, J.M.C. *Groundwater Contamination Inventory: A Methodological Guide*; IHP-VI Series on Groundwater No. 2; UNESCO: Paris, France, 2002.
75. Cao, W.; Bowden, W.B.; Davie, T.; Fenemor, A. Modelling impacts of land cover change on critical water resources in the Motueka River catchment, New Zealand. *Water Resour. Manag.* **2009**, *23*, 137–151. [[CrossRef](#)]
76. He, B.; Wang, Y.; Takase, K.; Mouri, G.; Razafindrabe, B.H. Estimating land use impacts on regional scale urban water balance and groundwater recharge. *Water Resour. Manag.* **2009**, *23*, 1863–1873. [[CrossRef](#)]
77. Kostyuchenko, Y.; Artemenko, I.; Abioui, M.; Benssaou, M. Global and Regional Climatic Modeling. In *Encyclopedia of Mathematical Geosciences*; Sagar, B.D., Cheng, Q., McKinley, J., Agterberg, F., Eds.; Springer: Cham, Switzerland, 2022; pp. 1–5. [[CrossRef](#)]

Disclaimer/Publisher’s Note: The statements, opinions and data contained in all publications are solely those of the individual author(s) and contributor(s) and not of MDPI and/or the editor(s). MDPI and/or the editor(s) disclaim responsibility for any injury to people or property resulting from any ideas, methods, instructions or products referred to in the content.